

MICRO-ABRASION WEAR TESTING OF MULTILAYER NANOCOMPOSITE TiAlSiN/TiSiN/TiAlN HARD COATINGS DEPOSITED ON THE AISI H11 STEEL

MIKROABRAZIJSKO PREIZKUŠANJE OBRABE VEČPLASTNE NANOKOMPOZITNE TRDE PREVLEKE TiAlSiN/TiSiN/TiAlN NA JEKLU AISI H11

Halil Çalişkan¹, Azmi Erdoğan¹, Peter Panjan², Mustafa Sabri Gök¹, Abdullah Cahit Karaoğlanlı¹

¹Bartın University, Faculty of Engineering, 74100 Bartın, Turkey

²Jožef Stefan Institute, Jamova 39, 1000 Ljubljana, Slovenia
halilcaliskan06@yahoo.com, hcaliskan@bartin.edu.tr

Prejem rokopisa – received: 2012-08-31; sprejem za objavo – accepted for publication: 2013-01-09

Nanostructured hard coatings are widely used to improve the wear resistance of tool steels in tribological applications. These coatings generally work under abrasive conditions and, therefore, a determination of their abrasive wear resistance has great importance. In this study, the free-ball micro-scale abrasion test, based on the ball-crater technique, has been used to evaluate the wear resistance of a multilayer nanocomposite nc-TiAlSiN/TiSiN/TiAlN hard coating. The coating was deposited on the AISI H11 cold-work tool steel using the industrial magnetron sputtering system. The microhardness and adhesion of the coating to the substrate were measured with the nanoindentation and scratch tests, respectively. The wear tests have been performed using SiC abrasive slurry on ball-cratering equipment. The crater-wear volumes have been evaluated using an optical microscope (OM). An analysis of the worn craters was conducted with a scanning electron microscope (SEM). It was found that the nc-TiAlSiN/TiSiN/TiAlN hard coating has a better adhesion to the AISI H11 steel substrate and a higher abrasive wear resistance than a conventional TiN coating. A two-fold increase in the sliding speed resulted in an approximately two-fold increase in the removed-wear volume. Three different wear mechanisms, i.e., micro-scratch, lateral fracture and plastic deformation, took place on the craters formed on the nc-TiAlSiN/TiSiN/TiAlN coated steel.

Keywords: nanocomposite hard coating, TiAlSiN/TiSiN/TiAlN, micro-scale abrasion wear, scratch test, tool steel

Nanostrukturirane trde prevleke se uporabljajo za izboljšanje obrabne odpornosti orodnih jekel za tribološko uporabo. Te prevleke navadno delujejo v razmerah abrazijske obrabe in je zato pomembno ugotavljanje njihove odpornosti proti abrazijski obrabi. V tej študiji je bil uporabljen mikroabrazijski preizkus s prosto kroglico, ki temelji na tehniki kraterja kroglice, za preizkus obrabne odpornosti trde prevleke iz večplastnega nanokompozita nc-TiAlSiN/TiSiN/TiAlN. Prevleka je bila nanosena na orodno jeklo za delo v hladnem AISI H11 z uporabo industrijskega magnetronskega sistema za naprščevanje. Mikrotreda in oprijemljivost na podlago sta bili izmerjeni z nanomerilnikom trdote in s preizkusom razenja. Preizkus obrabe je bil narejen z uporabo abrazijske suspenzije s SiC na napravi s kroglico. Volumen kraterja pri obrabi je bil ocenjen z uporabo svetlobnega mikroskopa (OM). Analiza kraterjev pri obrabi je bila narejena z vrstičnim elektronskim mikroskopom (SEM). Ugotovljeno je bilo, da ima trda prevleka nc-TiAlSiN/TiSiN/TiAlN boljšo oprijemljivost na podlagi iz jekla AISI H11 in boljšo odpornost proti obrabi kot navadna TiN-prevleka. Dvakratno povečanje hitrosti drsenja je povzročilo dvakratno povečanje volumna obrabe. Na kraterjih, ki so nastali na jeklu, prevlečenem z nc-TiAlSiN/TiSiN/TiAlN, so bili vidni trije mehanizmi obrabe: mikrorazenje, bočno drobljenje in plastična deformacija.

Ključne besede: nanokompozitna trda prevleka, TiAlSiN/TiSiN/TiAlN, abrazijska obraba na mikropodročju, preizkus razenja, orodno jeklo

1 INTRODUCTION

The AISI H11 hot-work tool steel is widely used in the production of mandrels, punchers, dies, moulds, knives and rollers. Despite the fact that different types of wear mechanisms such as fatigue and adhesive wear take place on these components, abrasion is one of the most important wear types. The friction occurring under working conditions necessitates the components to have a high hardness and wear resistance.¹ Therefore, thin film coatings of different materials (TiN, TiAlN, TiAlSiN, etc) have been developed and deposited on these steel components in order to prolong their lifetime in industry. The most important properties of these coatings are their much higher hardness and abrasive wear resistance compared to the uncoated substrates.²⁻⁶

The newly developed nc-TiAlSiN/TiSiN/TiAlN multilayer nanocomposite hard coating was found to be smooth and chemically stable, and it has low residual stresses and the maximum application temperature of 1100 °C.⁷ Therefore, the coating has a wide application area in industry. In order to improve the performance of the nc-TiAlSiN/TiSiN/TiAlN coating and to select the coating which is suitable for the applications mentioned above, a determination of its abrasive wear resistance is important.

The micro-abrasion wear test, introduced by Kassman et al.,⁸ is a widely used method for determining the abrasive wear resistance of thin hard coatings.^{2,9-11} In the test, a hardened ball is rotated on a sample under a certain load, with an addition of an abrasive slurry into the contact zone. Then, the crater track formed is

evaluated using profilometry and microscopy, and the wear characteristics are determined.¹² The test is easy to perform and very effective with respect to the wear resistance of the materials, and it needs only a small area of a sample. Therefore, in this study, the effect of the nc-TiAlSiN/TiSiN/TiAlN coating on the wear resistance of the AISI H11 steel was investigated using the micro-abrasion test. The adhesion of the coating on the substrate was determined and the wear behavior of the coating and the substrate was evaluated.

2 EXPERIMENTAL WORK

2.1 Substrate and the coating material

The test plates made of the AISI H11 tool steel with the diameter of 23 mm and the thickness of 1 mm were used as a substrate for the characterization and wear tests. The AISI H11 steel was quenched at 1150 °C and tempered at 560 °C to its final hardness of 931 HV. The heat treatment was performed in a vacuum furnace.

The industrial magnetron sputtering system CC800/9 sinOx ML (CemeCon) was used for depositing the nc-TiAlSiN/TiSiN/TiAlN coatings onto the test plates. The deposition system has four unbalanced magnetron sources placed on the corners of a rectangle. Two segmental TiSi and two segmental TiAl targets were used for depositing the nc-TiAlSiN/TiSiN/TiAlN coatings. The samples were moved in a two-fold rotation to obtain the nanoscale structures and also to ensure a constant film-thickness distribution on the substrates. The conventional TiN coating was also deposited on the H11 steel to make a comparison between the micro-abrasion

wear tests. The layer structures and thickness data for the coatings are shown in **Figure 1**. The thickness of the coatings was calculated from the craters formed with the ball-cratering technique (Calotest). It is seen that both coatings have a similar thickness (5.4 µm for the nc-TiAlSiN/TiSiN/TiAlN and 6.2 µm for the TiN coating).

2.2 Laboratory tests

The microhardness of the coatings on the AISI H11 substrates was measured with a Fisherscope H100C nanoindenter using a Vickers indenter at room temperature. The load increased stepwise and then decreased. From the loading/unloading curves, the indentation modulus $E^* = E/(1 - \nu^2)$ (where E and ν are Young's modulus and Poisson ratio, respectively)¹³ and hardness H of the coatings were calculated. The microhardness measurements were made at the maximum load of 50 mN for the coatings and at the maximum load of 1000 mN for the substrate. For a better reliability of the results, the measurements deviating significantly from the general trend in the load-displacement graph were deleted. The mean of the remaining values (typically around twenty) were determined as the hardness of the coatings.

The adhesion of the coatings to the substrates was investigated using a CSM Revetest scratch tester where a moving diamond stylus pressed along a sample surface with a progressive load. The radius of the diamond indenter used in the scratch test was 200 µm. The test parameters were selected as follows: the scratch length of 3 mm, the maximum load of 150 N, the loading rate of 200 N/min and the stylus speed of 4 mm/min. The load, which caused the chipping without an exposure of the substrate (the cohesive failure) at the track edges, was considered as the critical load of L_{C1} . The critical load of L_{C2} was determined with a complete removal of the coating in the scratch track. The critical load for the beginning of the coating chipping (L_{C1}) was determined with optical observation and acoustic emission. For the critical load of L_{C2} , friction-force recording was additionally used.

2.3 Micro-abrasion wear tests

The micro-abrasion wear tests were carried out using a free-ball cratering device in order to compare the abrasive wear resistance of the nc-TiAlSiN/TiSiN/TiAlN and conventional TiN coatings and the uncoated AISI H11 steel (**Figure 2**). The abrasive slurry composed of 25 g of SiC (1200 mesh) in 75 ml of water and a polished ball of AISI 52100 steel with the diameter of 25.4 mm were used. The ball rotation speeds were selected as 73.7 r/min and 147.4 r/min (corresponding to 0.099 m/s and 0.198 m/s, respectively). All the tests were performed within the duration of (300, 360 and 420) s, and they were repeated three times. The crater-wear

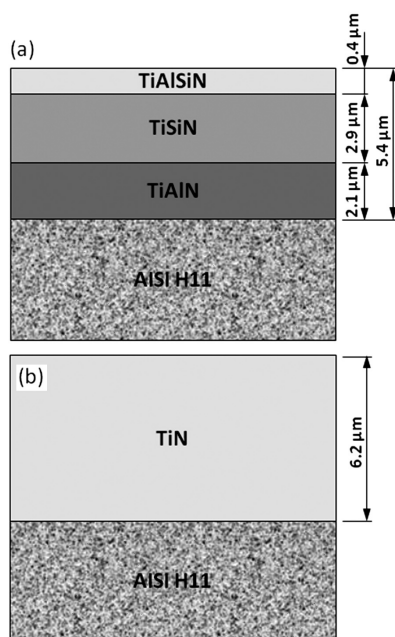


Figure 1: Layer structure and thickness data for: a) nc-TiAlSiN/TiSiN/TiAlN and b) TiN coating

Slika 1: Struktura plasti in podatki o debelini: a) nc-TiAlSiN/TiSiN/TiAlN in b) prevleka TiN

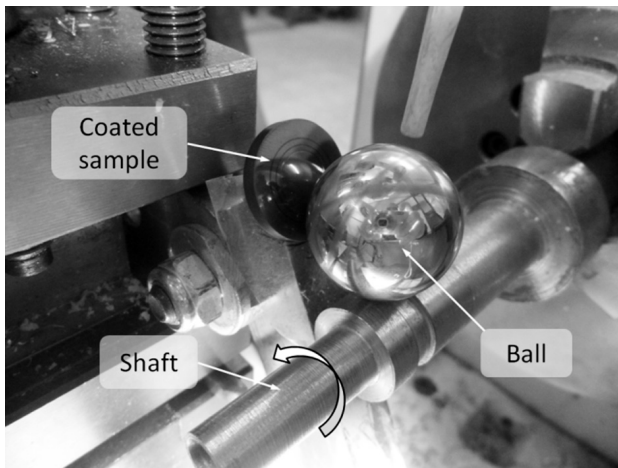


Figure 2: Free-ball micro-abrasion test device
Slika 2: Naprava za mikroabrazijski preizkus s prosto kroglico

volumes have been evaluated using an optical microscope and calculated using the equations from^{14,15}. The analysis of the worn craters was conducted with SEM.

3 RESULTS

3.1 Mechanical analysis

A comparison of the hardness and indentation modulus of the coatings and the substrate is given in

Table 1. The microhardness of the nc-TiAlSiN/TiSiN/TiAlN coating is 1.26 times higher than that of the TiN coating and 4.16 times higher than that of the substrate.

Table 1: Hardness and indentation modulus of the coatings and substrate

Tabela 1: Trdota in modul vtiskavanja prevlek in podlage

Material	H/HV	E*/GPa
nc-TiAlSiN/TiSiN/TiAlN	3869±387	361±21
TiN	3072±216	398±18
AISI H11	931±2	245±2

During the progressive scratch tests of the coatings, chipping, spalling, conformal cracking and buckling failures were observed.¹⁶ **Figure 3** shows images of the scratch tracks at L_{C1} and L_{C2} that occurred in the nc-TiAlSiN/TiSiN/TiAlN coating deposited onto the AISI H11 steel. The failures on the coating started with the angular cracks outside the tracks. The chippings formed at the edges of the tracks. Delamination of the TiAlSiN top layer or TiSiN layer was observed. The critical loads of L_{C1} and L_{C2} were measured as 41 N and 145 N, respectively. Thus, the nc-TiAlSiN/TiSiN/TiAlN coating exhibited a much better adhesion than the conventional single-layer TiN coating ($L_{C1} = 40$ N and $L_{C2} = 85$ N).

3.2 Micro-abrasion wear tests

The wear-coefficient graphs for the coated and uncoated samples obtained at the ball rotation speed of 147.4 r/min are given in **Figure 4**. Using the equations from^{14,15}, two different wear coefficients were calculated for the substrate and substrate + coating. The graph shows that the wear resistance of the AISI H11 steel was drastically improved by both the nc-TiAlSiN/TiSiN/TiAlN and TiN coatings, and the lowest wear coefficient was obtained with the nc-TiAlSiN/TiSiN/TiAlN coating. As seen from the graph, the wear coefficient of the nc-TiAlSiN/TiSiN/TiAlN coated sample slightly decreases with the sliding distance, while that of the TiN

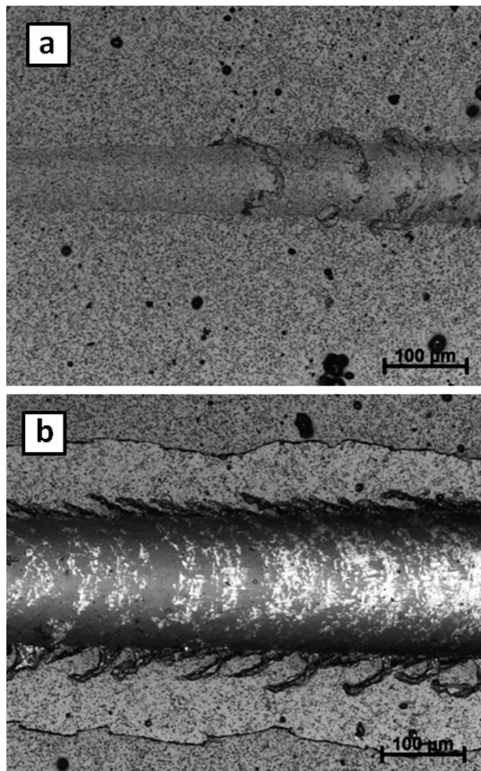


Figure 3: Scratch images of the nc-TiAlSiN/TiSiN/TiAlN coating on the AISI H11 substrate at the critical loads of: a) L_{C1} and b) L_{C2}
Slika 3: Slika raze na prevleki nc-TiAlSiN/TiSiN/TiAlN na podlagi AISI H11 pri kritičnih obremenitvah: a) L_{C1} in b) L_{C2}

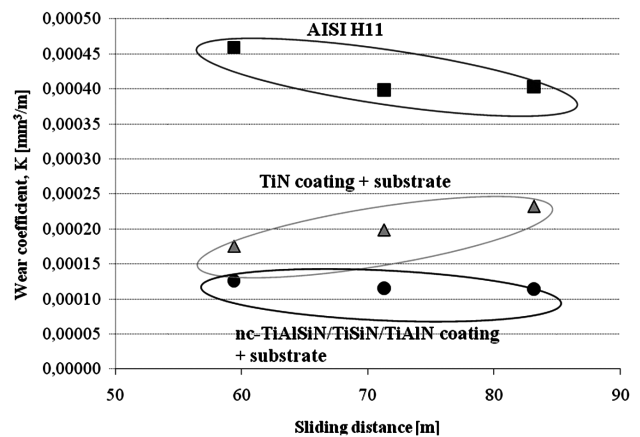


Figure 4: Wear coefficient as a function of sliding distance
Slika 4: Koeficient obrabe v odvisnosti od dolžine drsenja

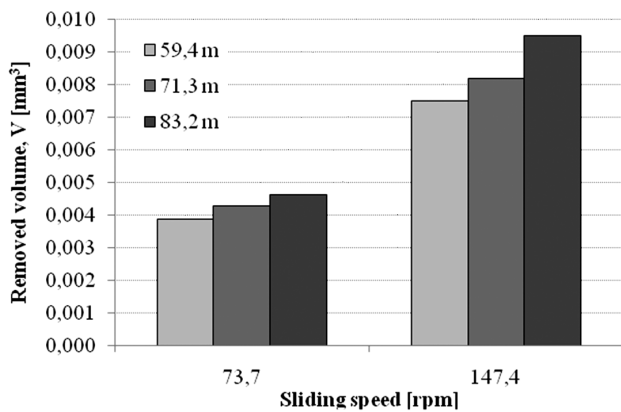


Figure 5: Effect of the sliding speed on the wear
Slika 5: Vpliv hitrosti drsenja na obrabo

coated one increases. This situation can be explained by concluding that at the beginning of the wear testing of both coatings the pressure applied on the abrasive SiC particles, and thus on the coated sample, is high (due to the point contact) causing a high wear rate. However, the pressure on the sample decreases with the increasing contact area during the sliding as a result of the wear. Owing to the high hardness and adhesion of the nc-TiAlSiN/TiSiN/TiAlN coating, a slight decrease in the wear coefficient was observed. On the other hand, in the case of the TiN coating, the coating was detached from the substrate due to the abrasion wear and a lower adhesion of the TiN coating to the AISI H11 steel and, therefore, the wear coefficient increased with the sliding distance.

In **Figure 5** the effect of the ball sliding speed on the removed volume is shown. Here, the tests were repeated at 73.7 r/min for the same sliding distance with the nc-TiAlSiN/TiSiN/TiAlN coating. A two-fold increase in the sliding speed resulted in an approximately two-fold increase in the removed wear volume. An increase in the ball rotation speed increased the peripheral speed of the SiC particles moved by the ball surface. Accordingly, more energy was applied onto the sample surface and more particles were removed from the coating and the substrate.

The image of the crater formed on the nc-TiAlSiN/TiSiN/TiAlN coating of the AISI H11 steel after the sliding distance of 83.2 m at the ball rotation speed of 147.4 r/min is shown in **Figure 6a**. It is seen that the crater has a well-defined circular shape that is the same for all the craters obtained. As seen from **Figures 6b** and **d**, the coating has shown quite a good adhesion to the substrate. It is possible to divide the wear on the crater into three different zones. The first one is the tearing that occurred at the top side of the crater (**Figure 6b**). Observing the SEM image, it can be concluded that it was caused by a plastic deformation of the coating material due to the cutting effect of the abrasive particles. The second wear is the rupture of the coating and the substrate material resulting from a locally exceeded plastic deformation of these materials in front of the abrasive SiC particles (**Figure 6c**). On the surface, the lateral-fracture wear mechanism was observed depending on a very small size of the abrasive particles. The third wear is the regularly spaced, parallel grooves that occurred at the bottom side of the crater where the abrasive slurry leaves the wear zone, as observed by

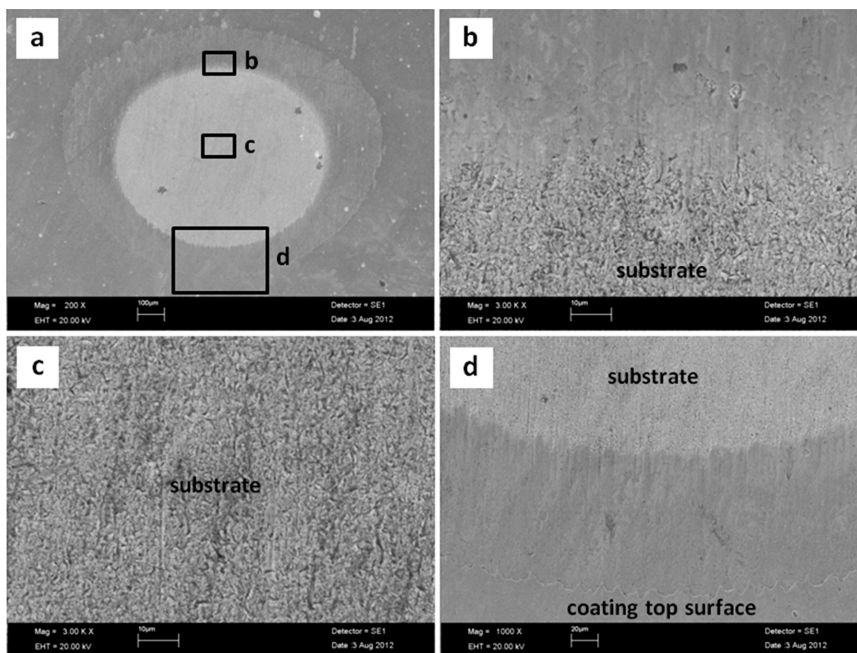


Figure 6: SEM images of a micro-abrasion crater on the nc-TiAlSiN/TiSiN/TiAlN coating after the sliding distance of 83.2 m
Slika 6: SEM-posnetki kraterja pri mikroabraziji na prevleki nc-TiAlSiN/TiSiN/TiAlN po 83,2 m drsenja

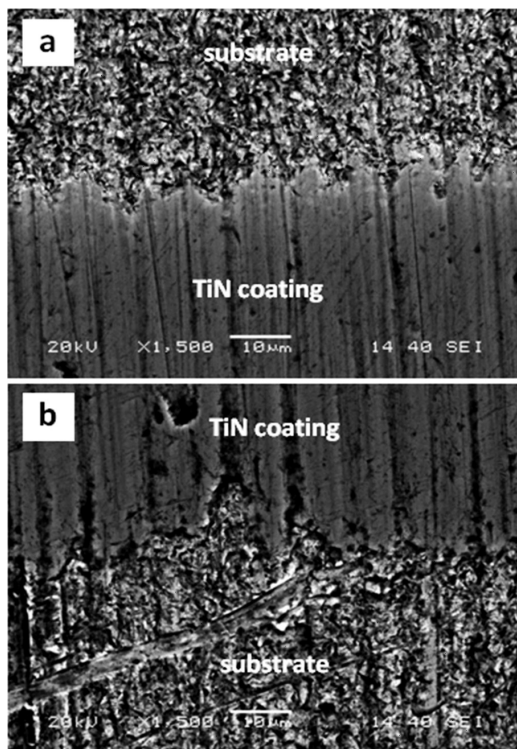


Figure 7: SEM images of the: a) bottom and b) top side of the micro-abrasion crater on the single-layer TiN coating after the sliding distance of 83.2 m

Slika 7: SEM-posnetka: a) dna in b) vrha kraterja pri mikroabraziji na enoplastnem sloju TiN po 83,2 m drsenja

Martinho et al.¹⁷ (Figure 6d). The difference between the wear mechanisms at the top and bottom sides of the crater can be due to the initial particle distribution in the contact inlet area. At the bottom side, the first grooves are drawn by the first particles embedded in the ball surface due to the two-body micro-abrasion wear mechanism, and the following particles follow the same trajectory.⁹ However, at the top side of the crater, the abrasive-slurry supply destroys the groove trajectory of the previous particles due to the three-body wear mechanism.

The images of the crater formed on the single-layer TiN coating of the AISI H11 steel after the sliding distance of 83.2 m at the ball rotation speed of 147.4 r/min are shown in Figure 7. It is clearly seen from the wear image that the regularly spaced, parallel, deep grooves form on the TiN coating and AISI H11 steel as a result of the sliding of the harder SiC particles due to a two-body micro-abrasion wear mechanism. Differently from the nc-TiAlSiN/TiSiN/TiAlN coating, these grooves exist at both the bottom (Figure 7a) and top sides (Figure 7b) of the crater on the TiN coating. The wear mechanisms at the top side of the crater on the nc-TiAlSiN/TiSiN/TiAlN coating were explained beforehand (Figure 6b). The reason for the difference in the wear mechanisms at the top sides of the craters on the compared coatings is probably that the micro-hardness of the TiN coating (3072 HV) is lower than that

of the nc-TiAlSiN/TiSiN/TiAlN coating (3869 HV). The TiN coating is easily worn by hard SiC particles and the forming grooves are deepened quickly. In addition, the lower adhesion of the TiN coating, compared to the nc-TiAlSiN/TiSiN/TiAlN coating, resulted in the detachments of the coating along the substrate-coating boundary and even in the wearing of the inner part of the coating. The wear mechanism on the AISI H11 steel is similar to that on the TiN coating due to the same reasons explained above (Figures 7a and b).

4 CONCLUSIONS

In the study, the effect of the nc-TiAlSiN/TiSiN/TiAlN hard coating on the abrasive-wear resistance of the AISI H11 steel was investigated using the free-ball abrasive-wear test and the following results were drawn:

The nc-TiAlSiN/TiSiN/TiAlN hard coating has a better adhesion to the AISI H11 steel substrate and a higher abrasive-wear resistance than the conventional TiN coating. The nc-TiAlSiN/TiSiN/TiAlN hard coating provides three times more micro-abrasive wear resistance than the uncoated AISI H11 substrate under the test conditions. A two-fold increase in the sliding speed results in an approximately two-fold increase in the removed-wear volume. Three different wear mechanisms – micro-scratch, lateral fracture and plastic deformation – take place on the craters formed on the nc-TiAlSiN/TiSiN/TiAlN coated AISI H11 steel.

5 REFERENCES

- M. B. Karamış, K. Yıldızlı, G. Çarkıt Aydın, Sliding/rolling wear performance of plasma nitrided H11 hot working steel, *Tribology International*, 51 (2012), 18–24
- X. Z. Ding, C. T. Bui, X. T. Zeng, Abrasive wear resistance of Ti_{1-x}Al_xN hard coatings deposited by a vacuum arc system with lateral rotating cathodes, *Surface and Coatings Technology*, 203 (2008) 5–7, 680–684
- J. Richter, Micro-scale abrasion testing of PVD TiN coatings on conventional and nonledeburitic high-speed steels, *Wear*, 257 (2004) 3–4, 304–310
- H. Çalışkan, C. Kurbanoglu, P. Panjan, D. Kramar, Investigation of the performance of carbide cutting tools with hard coatings in hard milling based on the response surface methodology, *The International Journal of Advanced Manufacturing Technology*, 66 (2013), 5–8, 883–893
- M. G. Faga, G. Gautier, R. Calzavarini, M. Perucca, E. A. Boot, F. Cartasegna, L. Settineri, AlSiTiN nanocomposite coatings developed via Arc Cathodic PVD: Evaluation of wear resistance via tribological analysis and high speed machining operations, *Wear*, 263 (2007) 7–12, 1306–1314
- H. Çalışkan, C. Kurbanoglu, D. Kramar, P. Panjan, J. Kopač, Hard milling operation of AISI O2 cold work tool steel by carbide tools protected with different hard coatings, *Engineering Science and Technology: An International Journal (JESTECH)*, 15 (2012) 1, 21–26
- F. Klocke, F. Quito, K. Arntz, A. A. Souza, C. Ader, Investigation of tool geometry, coating and coolant in micro milling of single crystal Nickel-based superalloy René N5, in: 3rd CIRP International Conference on High Performance Cutting, Dublin-Ireland, 2008, 561–574

- ⁸ Å. Kassman, S. Jacobson, L. Erickson, P. Hedenqvist, M. Olsson, A new test method for the intrinsic abrasion resistance of thin coatings, *Surface and Coatings Technology*, 50 (1991) 1, 75–84
- ⁹ M. F. C. Andrade, R. P. Martinho, F. J. G. Silva, R. J. D. Alexandre, A. P. M. Baptista, Influence of the abrasive particles size in the micro-abrasion wear tests of TiAlSiN thin coatings, *Wear*, 267 (2009) 1–4, 12–18
- ¹⁰ J. C. A. Batista, C. Godoy, A. Matthews, Micro-scale abrasive wear testing of duplex and non-duplex (single-layered) PVD (Ti,Al)N, TiN and Cr–N coatings, *Tribology International*, 35 (2002) 6, 363–372
- ¹¹ D. N. Allsopp, I. M. Hutchings, Micro-scale abrasion and scratch response of PVD coatings at elevated temperatures, *Wear*, 251 (2001) 1–12, 1308–1314
- ¹² M. J. Ibáñez, J. Gilabert, M. Vicent, P. Gómez, D. Muñoz, Determination of the wear resistance of traditional ceramic materials by means of micro-abrasion technique, *Wear*, 267 (2009) 11, 2048–2054
- ¹³ W. C. Oliver, G. M. Pharr, An improved technique for determining hardness and elastic modulus using load and displacement sensing indentation experiments, *Journal of Materials Research*, 7 (1992), 1564–1583
- ¹⁴ K. I. Schiffmann, R. Bethke, N. Kristen, Analysis of perforating and non-perforating micro-scale abrasion tests on coated substrates, *Surface and Coatings Technology*, 200 (2005) 7, 2348–2357
- ¹⁵ I. M. Hutchings, Abrasive and erosive wear tests for thin coatings: a unified approach, *Tribology International*, 31 (1998) 1–3, 5–15
- ¹⁶ S. J. Bull, Failure mode maps in the thin film scratch adhesion test, *Tribology International*, 30 (1997) 7, 491–498
- ¹⁷ R. P. Martinho, M. F. C. Andrade, F. J. G. Silva, R. J. D. Alexandre, A. P. M. Baptista, Micro-abrasion wear behaviour of TiAlCrSiN nanostructured coatings, *Wear*, 267 (2009) 5–8, 1160–1165